Design and Development of Radio Tomographic Imaging System

C. C. Lee[1], M. H. F. Rahiman[1,2*], R. A. Rahim[3] and F. S. A. Saad[1,2]

[1] Faculty of Electrical Engineering Technology, Universiti Malaysia Perlis, Pauh Putra Campus, 02600 Arau, Perlis, Malaysia.
[2*] Centre of Excellence for Advanced Sensor Technology (CEASTech), Universiti Malaysia Perlis (UniMAP), Perlis, Malaysia.
[3] School of Electrical Engineering, Faculty of Engineering, Universiti Teknologi Malaysia, 81310 Skudai, Johor, Malaysia.

Corresponding author* email: hafiz@unimap.edu.my
Accepted 3 March 2021, available online 31 March 2021

ABSTRACT

Radio tomographic imaging (RTI) is an emerging imaging technique that utilizes the shadowing losses on links between multiple pairs of wireless nodes within the monitoring area to estimate the attenuation of physical objects. In recent years, RTI has gained huge interest from the researchers in device-free localization (DFL) field due to its ability in generating an image to localize a target within the monitoring area. From the literature studies, researchers are primarily focused on the study of characterizing RSSI attenuation for different purposes such as human presence detection, privacy-preserving localization, indoor and outdoor localization. However, to the best of the authors' knowledge, there is no research conducted in studies the effects of phantoms with different dimensions towards the changes in received signal strength indicator (RSSI) value. Therefore, this paper presents a design and development of the RTI system to study and characterize the behaviour of radio waves propagation when phantoms with different dimensions are present within the monitoring area. An overview of the proposed RTI system, the arrangement of sensor arrays and a few factors that should take into consideration when using the RF sensors such as ground effects, near field and far-field region of an antenna have been discussed in this paper. Also, the details of the experimental design have been explained. Based on the results obtained from the experiments, the RSSI value decreases gradually as the dimension of phantoms with water medium increases. This is because when the diameter of a phantom with water medium increased, the water content inside the phantom also increased. Also, water is a high-attenuating medium and its dielectric constant is 80. Therefore, when the diameter of a phantom with water medium increased, the energy of the EM waves is absorbed and scattered more. This caused the attenuation of EM waves increased and resulted in lower RSSI value.

Keywords: Radio tomographic imaging, received signal strength indicator, sensor arrays

1. Introduction

Radio Tomographic Imaging (RTI) is an emerging imaging technique that utilizes the shadowing losses on links between multiple pairs of wireless nodes within the monitoring area to estimate the attenuation of physical objects. The shadowing losses is referred to the variations in the received signal strength (RSS) measurements which will be used to reconstruct a tomographic image. The tomographic image provides information about the shape, size and position of an object. Figure 1(a) shows an illustration of the wireless sensor network (WSN) in the RTI system[1], [2]. The black colour dots represent the radio frequency (RF) sensors that operate in transceivers mode. When the RTI system is operating, the transceivers in the sensor network will communicate with each other and formed a unique link. The object that enters the monitoring area at this time will absorb, diffract, reflect, or scatter some of the transmitted waveforms. Also, at the same time, the object will block some of the lines of sight (LOS) path. This caused the links between multiple pairs of RF nodes to experience shadowing losses. Figure 1(b) shows an object which blocks the LOS path of the unique links in the RTI system[1], [2].

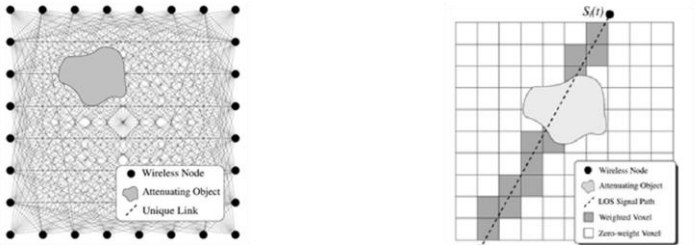

(a) (b)

Figure. 1. An illustration of (a) the wireless sensor network in the RTI system, (b) LOS path and the object in the RTI system.

In recent years, RTI has gained huge interest from the researchers in the device-free localization (DFL) field. RTI is capable in generating an image to localize stationary and moving targets within the monitoring area using the RSS measurements only without any phase and timing information[1], [3]–[16]. However, the process of reconstructing a tomographic image from the RSS measurements is an ill-posed inverse problem. Consequently, a small number of errors or variations in sensor measurements will lead to a significant impact on the image quality[1], [2], [17], [18]. Therefore, it is crucial to study the effects on the RSS measurements between the transceivers when their LOS paths in the RTI system are blocked by different dimensions of phantoms.

From the literature studies, researchers are primarily focused on the study of characterizing RSSI attenuation for different purposes such as human presence detection[19], privacy-preserving localization[1], [11], [20], indoor and outdoor localization[11], [21], [22]. Apparently, when there is no object presence detected within the monitoring area, the RSSI values will be uniform with a small variation due to the measurement noise[2]. The RSSI values will drop significantly whenever the object presents within the monitoring area. However, to the best of the authors' knowledge, there is no research conducted in studies the effects of phantoms with different dimensions towards the changes in received signal strength indicator (RSSI) value. Therefore, in this paper, an RTI system is designed and developed to characterize the behaviour of radio waves propagation when phantoms with different dimensions are present within the RTI system.

2. Methodology

The design and development of the RTI system divided into two subsections, which are the sensor arrays arrangement and projection geometry. The sensor arrays arrangement section described an overview of the proposed RTI system, the arrangement of sensor arrays and a few factors that should take into consideration when using the RF sensor. In section 2.2, the details of the proposed fan-shaped beam projection and transceiver operation were explained.

2.1 Sensor Arrays Arrangement

Figure 2 shows an overview of the proposed RTI system. The proposed system was designed with 8 units of 2.4GHz RF sensors that perform transceiver operation. For the initial study, the 8-RF sensors are mounted around the monitoring column intensively as a ring to evaluate the behaviour of radio waves propagation when phantoms with different dimensions are present within the monitoring area. The RF sensors are placed at an equal distance from each other by 45° and from the centre of monitoring column. They are arranged in such a way to receive scattered electric field from multiple directions. The mathematical specification calculation of the model is as below.

$$Circumference = 2\pi r = 2*3.1416*50cm = 314.1593cm \quad (1)$$

$$Degree\ of\ rotation = 360/8 = 45\ degree \quad (2)$$

$$Angle\ sector = (45\pi/180)(50cm) = 39.2699cm \quad (3)$$

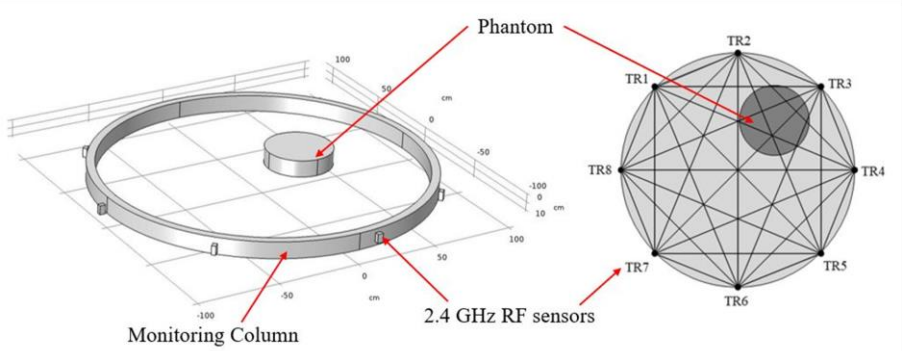

Figure. 2. An overview of the proposed RTI system.

Apart from that, there are a few factors that should be taken into consideration when using 2.4GHz RF sensors such as the ground reflection effects, near field and far-field region of an antenna[23][24]. This is because the radio waves propagation in the RTI system might be affected by the outside noise, the temperature in the surrounding, objects in the Fresnel region and interferences from other RF sources. Fresnel region is an ellipsoid shape area that includes radiated energy. The more obstacles within the Fresnel region, the more wave reflections will be created, which can lead to the received power losses. Therefore, to avoid signal degradation and power loss from the transmitter to the receiver, the position of the RF sensors is as important as its height above the ground. The radius of the Fresnel region can be calculated using formulae (4):

$$\textit{Radius of Fresnel Region, } r = 17.32\sqrt{\frac{d}{4f}} \qquad (4)$$

where r is the radius of Fresnel region in meters, d is the distance between antennas in kilometers, and f is the frequency in GHz. Figure 3 shows an illustration of the Fresnel region[25].

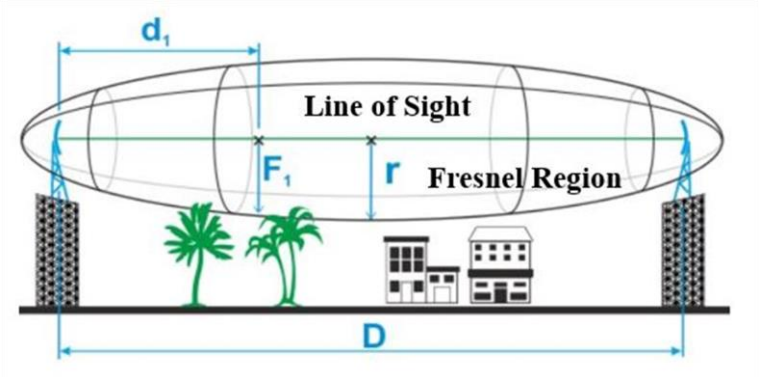

Figure. 3. An illustration of Fresnel region.

When the RF signals are transmitted from the radiation source to a receiver, the electromagnetic waves will effectively spread out as its distance increases. The characteristics of the electromagnetic (EM) field in the region close to the antenna are vary from the EM field in the region that far from the antenna. The fields surrounding an antenna are divided into three regions, which are reactive near field, radiating near field (Fresnel region) and far-field (Fraunhofer region) as shown in Figure 4[26], [27]. Since the antennas are usually used to transmit signals at a vast distance, therefore the far-field region is the most important as it is the region of operation for most antennas[26]. Besides, the radiation pattern of an antenna can be measured in the far-field region. To measure the radiation pattern of an antenna, it is important to choose a distance that large enough to be in the far-field region. This distance can be measured using formulae (5):

$$\textit{Far-Field Region, } r_{min} = \frac{2D^2}{\lambda} \qquad (5)$$

where r_{min} is the minimum distance from the antenna, D is the largest dimension of antenna and λ is the wavelength. Although the EM fields are largely unpredicted in the near field region and there is no measurements are usually made in that region; however, the distance of the near field region still need to be considered when attaching the RF sensors on the monitoring column. The distance of reactive and radiating near field can be calculated using formulae (6) and (7):

$$Reactive\ Near\ Field\ Region \leq 0.62 \times \sqrt{\frac{D^3}{\lambda}} \quad (6)$$

$$Radiating\ Near\ Field\ Region \leq \frac{2D^2}{\lambda} \quad (7)$$

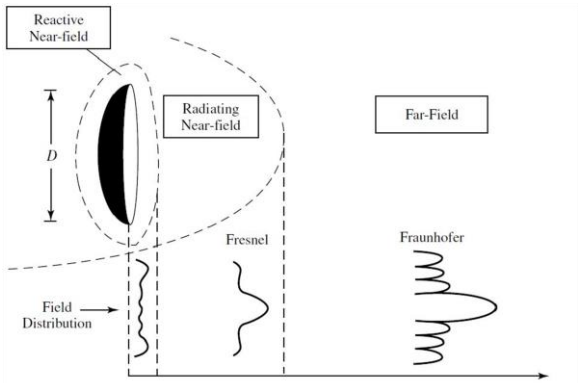

Figure. 4. Near and far field regions of an antenna.

2.2 Projection Geometry

In this study, a fan-shaped beam projection was used to obtain as much information as possible from each interrogation for producing a higher quality image. Figure 5(a) shows a single layer of fan-shaped beam projection. When all the single layer of projections from the 8-RF sensors are combined, it forms an RTI network as shown in Figure 5(b).

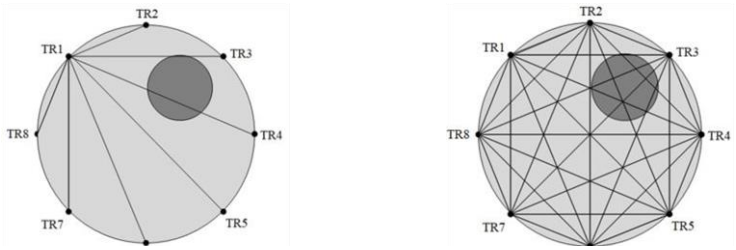

(a) (b)

Figure. 5. (a) Single layer of fan-shaped beam projection, (b) Multiple layers of fan-shaped beam projections that form an RTI network.

Apart from that, a transceiver operation is proposed in this study to increase the number of sensor measurements. In transceiver operation, each of the RF sensors can transmit and receive radio waves sequentially. When the RF sensor (TR1) operates as a transmitter, it will send the signals to the rest of the RF sensors (TR2-TR8). The 7-units of RF sensors (TR2-TR8) operate as a receiver and obtain the measurements from the transmitter (TR1). In each scanning process, RF sensor (TR1) will start the first data transmission, followed by the RF sensor (TR2) until all the RF sensors completed the transmission round before the next scanning continues. All the collected sensor measurements will be stored directly in the PC as shown in Figure 6.

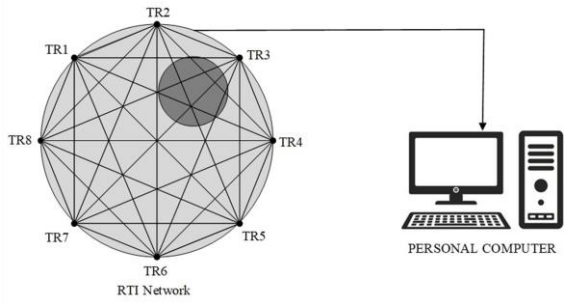

Figure. 6. Data acquisition system.

3. Design of Experiments

As discussed in Section 1.0, RTI is an imaging technique that utilizes the shadowing losses on links between the transmitter and receiver within the monitoring area to estimate the shape, size and position of an object. However, the process of reconstructing a tomographic image from the RSS measurements is an ill-posed inverse problem, meaning that a small number of variations in sensor measurements will lead to a significant impact on the image quality. Therefore, it is crucial to study the effects on the radio waves propagation within the monitoring area when the LOS paths in the RTI system are blocked by different dimensions of phantoms.

For the initial study, five phantoms with different diameters that range from 38cm to 11cm are used. The details of the phantoms' dimension are as illustrated in Table 1. For better characterization on the behaviour of radio waves propagation when phantoms with different diameters are present within the monitoring area, an experiment has been conducted to study:

i. The changes in RSSI values when the presence of phantom is not detected within the monitoring area
ii. The changes in RSSI values when the presence of phantom is detected within the monitoring area
iii. The changes in RSSI values when phantom with different diameters are present within the monitoring area

Apart from that, the phantoms used in the experiment contains two types of medium, which are air and water medium. As generally known, EM waves travel through free space. However, when it travels through the medium, the EM waves are attenuated as part of its energy is absorbed and scattered[28]. While the attenuation level of EM waves depends on the dielectric constant of the medium. Based on the literature studies, the dielectric constant of a vacuum is considered to be 1.0 and of air is approximately 1.0[29]. While the dielectric constant of water is 80[29]. Since the EM waves travel through free space, therefore, air medium was used in this study to evaluate the radio waves propagation in a normal state (without the presence of phantom). To characterize the radio waves propagation when the phantom with different dimensions are present within the monitoring area, a phantom with water medium was used in this study as it is a high attenuating medium.

Figure 7 shows an experimental setup for the RTI system. The experiment was carried out by placing the phantom (with air/water medium) at certain coordinates within the monitoring column to study the behaviour of radio waves propagation when the phantom blocked LOS paths between the transmitter and receiver. Also, to study the relationship between the diameter of phantom and the changes in RSSI value, only one phantom is used for each experiment. Since the five different diameters of phantoms used in this study consisted of air and water medium, therefore, 12 experiments were carried out. The water level inside the phantoms with the water medium is as the height of the monitoring column, which is 10cm. Table 2 shows the details of phantom profiles information where five different diameters of phantoms are placed at coordinate (3,4) within the monitoring area. The experiment was repeated by placing the phantoms at another two different coordinates within the monitoring area, which are coordinates (4,7) and (5,3). Therefore, a total number of 36 experiments were carried out.

Table 1. Dimension details of phantoms.

Phantoms	Dimension (Ø x h)	Medium of Phantoms	Material of Phantoms
A	38cm x 47.5cm	air and water	Plastic
B	29cm x 43cm	air and water	Plastic
C	22.5cm x 23cm	air and water	Plastic
D	15cm x 19cm	air and water	Plastic
E	11cm x 17cm	air and water	Plastic

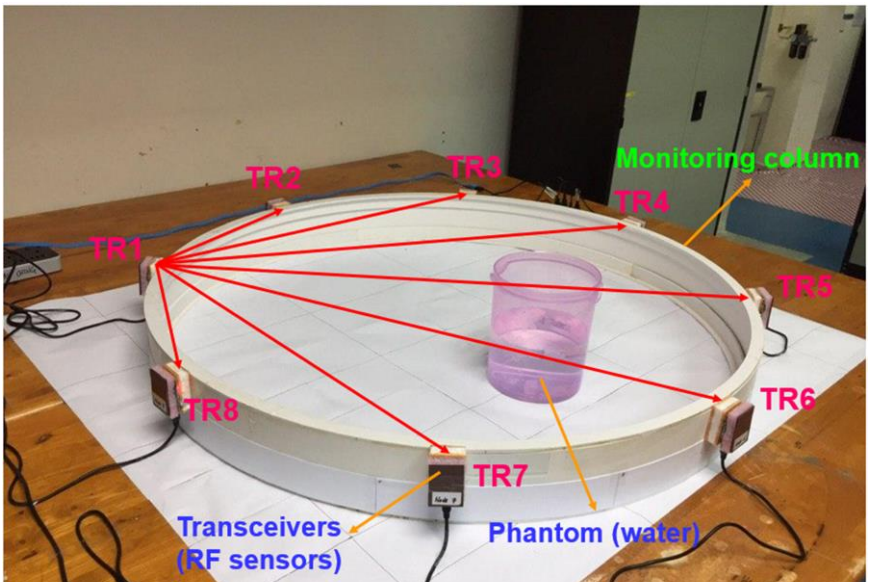

Figure. 7. Experimental setup for RTI system.

Table 2. Phantom profiles information.

Phantom A	Phantom B	Phantom C
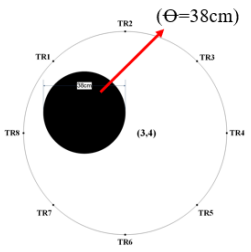	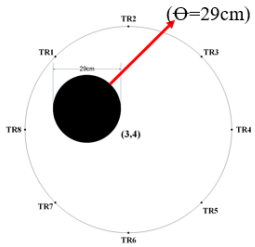	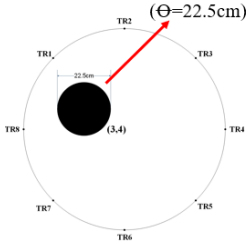
Phantom D	**Phantom E**	**Phantom F**
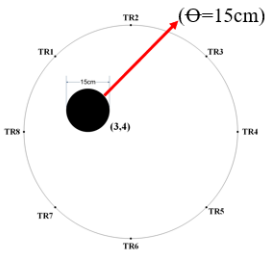	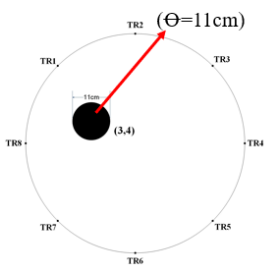	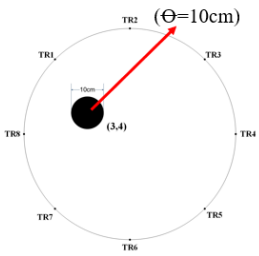

4. Results and Discussions

In this section, the results are presented in three subsections. The first section will discuss the RSSI measurement when there is no phantom presence within the monitoring area. Secondly, the changes in RSSI measurement when the phantom with air medium is present will be studied. The last subsection will be on the analysis of phantom with different diameters towards the reading of RSSI value.

4.1 Zero Phantom Presence

In order to differentiate and characterize the radio waves propagation with and without the presence of phantom within the monitoring area, the RSSI calibration data for each transmitter must be determined. In this study, 8-RF sensors were operated in transceiver mode, therefore, eight sets of RSSI calibration data were identified.

Table 3 shows the RSSI measurement when there is no phantom presence. Theoretically, the nodes that located at the opposite position will have similar signal strength. Based on the results in Table 3, the nodes that located in the opposite direction when the transmitter TR1 are operating, namely TR1_4 & TR1_6 have a similar RSSI value. However, the TR1_2 & TR1_8 and TR1_3 & TR1_7 have different RSSI value. Also, in theory, when the distance between transmitter and receiver increases, the signal strength between them will decreases which result in lower RSSI value. Both TR1_5 and TR3_7 which having the longest distance contain the lowest signal strength. Apart from that, theoretically, transmitters TR1 and TR3 that located in the opposite direction should have similar signals trends. However, based on the results shown in Table 3, the signals trends between TR1 and TR3 is different. This is due to environmental noises such as the temperature and objects in the surrounding. Therefore, it is crucial to study the behaviour of radio waves propagation for each transmitter as they will be affected by the noises in the surrounding and caused them to have different signals trends.

Table 3. The RSSI measurement with zero phantom presence (dBm).

Transmitters	Phantom Profiles	RSSI Measurement with Zero Phantom Presence (dBm)
TR1	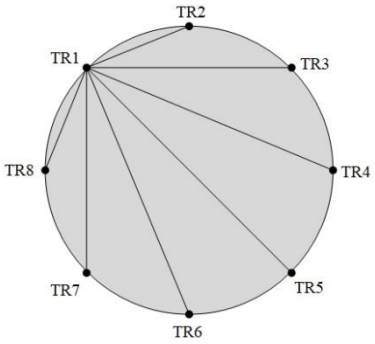	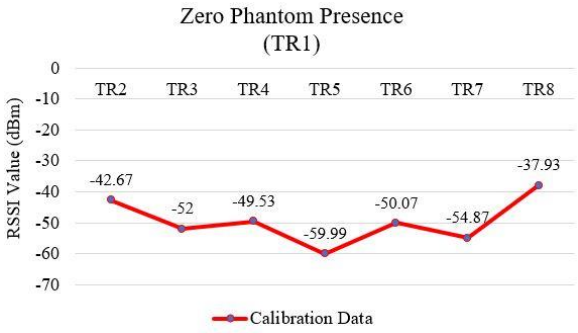
TR3	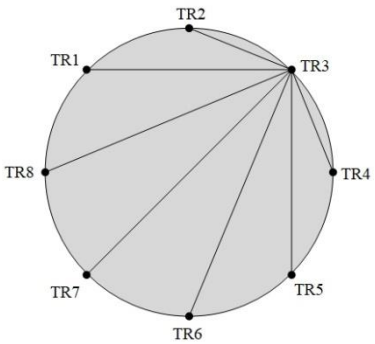	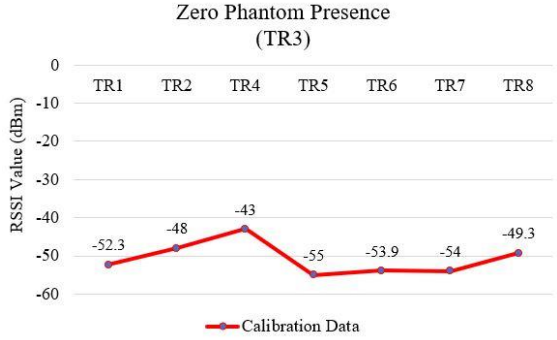

4.2 Evaluation of the Changes in RSSI Measurement when the Phantom with Air Medium is Present

Table 4.2 shows the changes in RSSI measurement when the phantoms with air medium are present within the monitoring area. Based on the results obtained, it is shown that the RSSI measurement when zero phantom and phantom with air medium presence within the monitoring area are similar. The material of the phantoms is made up of plastic and its dielectric constant is 4.0. Since the dielectric constant of the phantom is low, the EM waves able to pass through the

phantom easily and resulted in lower attenuation. Therefore, the RSSI value when zero phantom and phantom with air medium presence within the monitoring area are similar.

Table 4. The changes in RSSI measurement when the phantom with air medium is present (dBm).

Transmitters	Phantom Profiles	The Changes in RSSI Measurement when the Phantom with Air Medium is Present
TR1	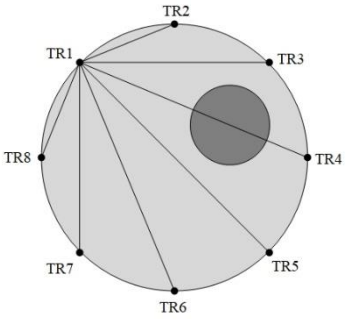	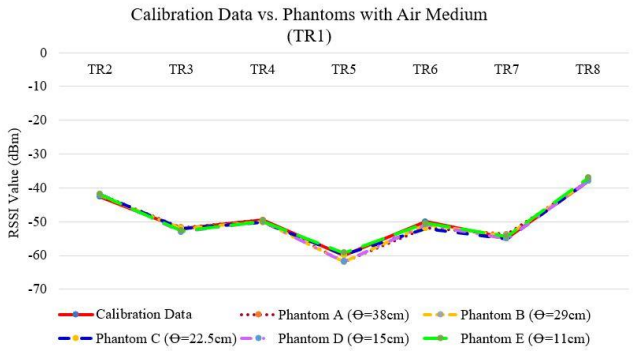
TR3	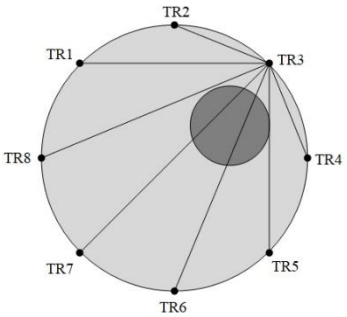	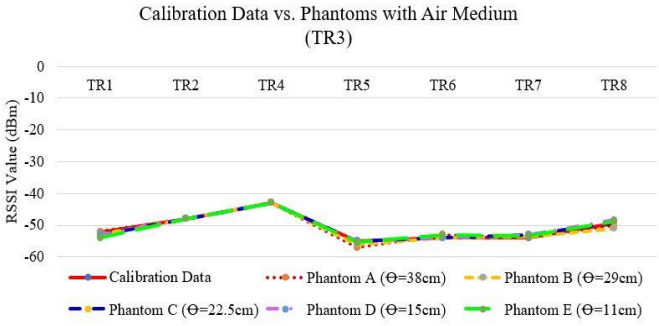

4.3 Evaluation on the Effects of Phantoms with Different Diameters Towards the Radio Waves Propagation

Table 5 shows the changes in RSSI measurement when the phantoms with water medium are present within the monitoring area. As shown in Table 5, when the TR1 is operating as a transmitter, it will transmit the signals to the rest of the receivers (TR2-TR8) and formed multiple unique links. However, the phantom that located at coordinate (5,3) within the monitoring area had blocked the LOS paths between TR1 and TR4. This had caused the links between TR1 and TR4 to experience shadowing losses which resulted in the variations of RSS measurements. From the results obtained, it can be seen that the RSSI value decreases gradually as the dimension of phantoms increases. Figure 8 shows the relationship between the diameter of phantoms and RSSI measurements in node TR1_4. Phantom A (Θ=38cm) experience the highest shadowing losses where its RSSI value has the lowest reading which is -56dBm. While Phantom E with the smallest dimension (Θ=11cm) experience the lowest shadowing losses where its RSSI value is -51.733dBm. When the diameter of a phantom with water medium increased, the water content inside the phantom also increased. Also, as mentioned in Section 3.0, water is a high-attenuating medium and its dielectric constant is 80. Therefore, when the diameter of a phantom with water medium increased, the energy of the EM waves is absorbed and scattered more. This caused the attenuation of EM waves increased and resulted in lower RSSI value.

Apart from that, based on the results of the experiment, there is one notable finding where the LOS path of monitoring links blocked by the phantoms not necessarily experience shadowing losses. The shadowing losses might be experienced by the other monitoring links that nearby. This is due to the reflection, absorption, diffraction and scattering of radio waves propagation[30]. Practically, the radio waves are not travelling in a straight-line form. Based on the phantom profiles of TR3, the LOS path of monitoring links TR3_7, TR3_6 and TR3_5 are blocked by the phantoms. Theoretically, the monitoring links TR3_7, TR3_6 and TR3_5 will experience shadowing losses. However, the obtained results showed that monitoring links TR3_1, TR3_5 and TR3_8 experience shadowing losses.

Table 5. The changes in RSSI measurement when the phantoms with water medium is present (dBm).

Transmitter	Phantom Profiles	The Changes in RSSI Measurement when the Phantom with Water Medium is Present
TR1	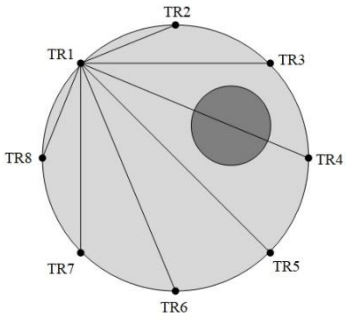	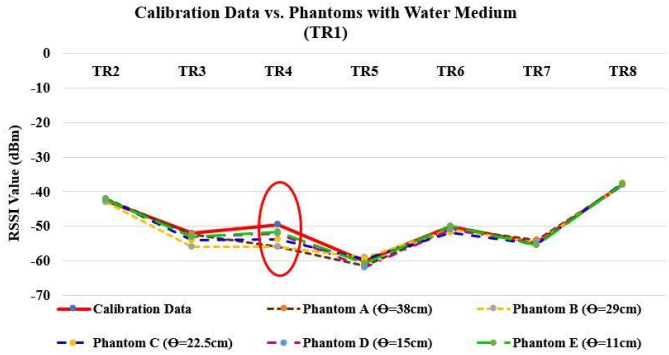
TR3	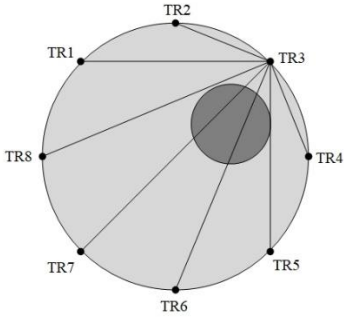	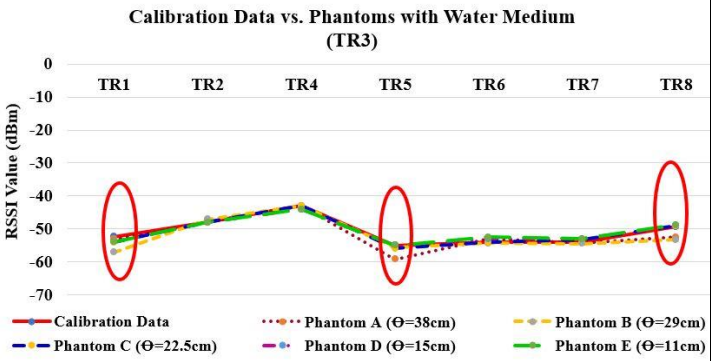

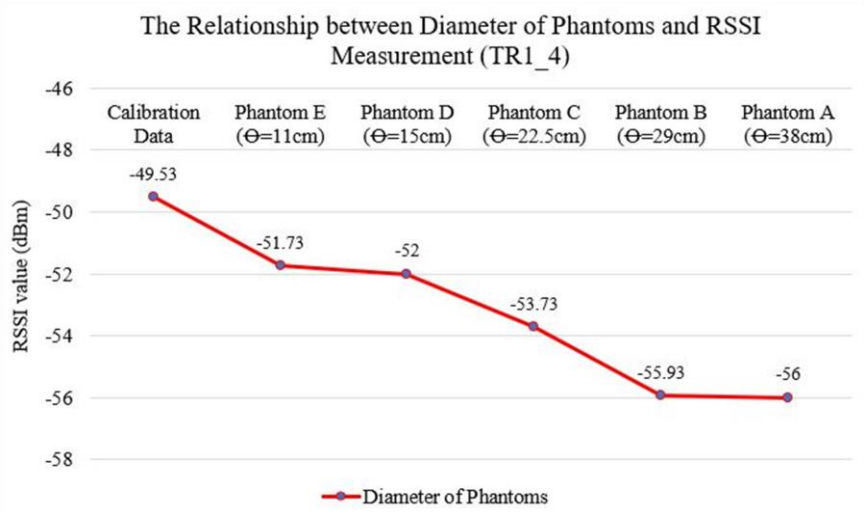

Figure. 8. The relationship between the diameter of phantoms and RSSI measurements.

5. Conclusions and Future Works

This paper presents a design and development of the RTI system to study and characterize the behaviour of radio waves propagation when phantoms with different dimensions are present within the monitoring area. An overview of the proposed RTI system, the arrangement of sensor arrays and a few factors that should take into consideration when using the RF sensors such as ground effects, near field and far-field region of an antenna have been discussed in this paper. Also, the details of the experimental design have been explained. Based on the results obtained from the experiments, the RSSI value decreases gradually as the dimension of phantoms with water medium increases. This is because when the diameter of a phantom with water medium increased, the water content inside the phantom also increased. Also, water is a high-attenuating medium and its dielectric constant is 80. Therefore, when the diameter of a phantom with water

medium increased, the energy of the EM waves is absorbed and scattered more. This caused the attenuation of EM waves increased and resulted in lower RSSI value. In the future, a study will be carried out to evaluate the radio waves propagation when several phantoms with different dimensions are present within the monitoring area.

Acknowledgement

This research was financed by the Collaboration Research Grant UTM-UniMAP 2018 (Grant No. 9023-00002). The authors gratefully thank Universiti Malaysia Perlis (UniMAP) for the facilities and technical support.

References

[1] J. Wilson and N. Patwari, "Radio tomographic imaging with wireless networks," *IEEE Trans. Mob. Comput.*, vol. 9, no. 5, pp. 621–632, 2010, doi: 10.1109/TMC.2009.174.

[2] J. Wilson, N. Patwari, and F. G. Vasquez, "Regularization Methods for Radio Tomographic Imaging," *2009 Virginia Tech Symp. Wirel. Pers. Commun.*, no. March 2014, 2009.

[3] N. Pirzada, M. Y. Nayan, F. S. M. F. Hassan, and M. A. Khan, "Device-free Localization Technique for Indoor Detection and Tracking of Human Body: A Survey," *Procedia - Soc. Behav. Sci.*, vol. 129, no. January 2016, pp. 422–429, 2014, doi: 10.1016/j.sbspro.2014.03.696.

[4] M. Bocca, O. Kaltiokallio, N. Patwari, and S. Venkatasubramanian, "Multiple target tracking with rf sensor networks," *IEEE Trans. Mob. Comput.*, vol. 13, no. 8, pp. 1787–1800, 2014, doi: 10.1109/TMC.2013.92.

[5] M. Bocca, A. Luong, N. Patwari, and T. Schmid, "Dial it in: Rotating RF sensors to enhance radio tomography," *2014 11th Annu. IEEE Int. Conf. Sensing, Commun. Networking, SECON 2014*, pp. 600–608, 2014, doi: 10.1109/SAHCN.2014.6990400.

[6] O. Kaltiokallio, M. Bocca, and N. Patwari, "Enhancing the accuracy of radio tomographic imaging using channel diversity," *MASS 2012 - 9th IEEE Int. Conf. Mob. Ad-Hoc Sens. Syst.*, pp. 254–262, 2012, doi: 10.1109/MASS.2012.6502524.

[7] O. Kaltiokallio, M. Bocca, and N. Patwari, "A fade level-based spatial model for radio tomographic imaging," *IEEE Trans. Mob. Comput.*, vol. 13, no. 6, pp. 1159–1172, 2014, doi: 10.1109/TMC.2013.158.

[8] D. K. Noh, L. Wang, Y. Yang, H. K. Le, and T. Abdelzaher, *Compressed RF Tomography for wireless sensor networks: centralized and decentralized approaches*, vol. 5516 LNCS. 2009.

[9] K. S. Anusha, R. Ramanathan, and M. Jayakumar, "Device free localisation techniques in indoor environments," *Def. Sci. J.*, vol. 69, no. 4, pp. 378–388, 2019, doi: 10.14429/dsj.69.13214.

[10] O. Kaltiokallio, M. Bocca, and N. Patwari, "Follow @grandma: Long-term device-free localization for residential monitoring," *Proc. - Conf. Local Comput. Networks, LCN*, pp. 991–998, 2012, doi: 10.1109/LCNW.2012.6424092.

[11] M. Bocca, O. Kaltiokallio, and N. Patwari, "Radio tomographic imaging for ambient assisted living," *Commun. Comput. Inf. Sci.*, vol. 362 CCIS, pp. 108–130, 2013, doi: 10.1007/978-3-642-37419-7_9.

[12] M. Khaledi, S. K. Kasera, N. Patwari, and M. Bocca, "Energy efficient radio tomographic imaging," *2014 11th Annu. IEEE Int. Conf. Sensing, Commun. Networking, SECON 2014*, pp. 609–617, 2014, doi: 10.1109/SAHCN.2014.6990401.

[13] S. Nannuru, Y. Li, Y. Zeng, M. Coates, and B. Yang, "Radio-frequency tomography for passive indoor multitarget tracking," *IEEE Trans. Mob. Comput.*, vol. 12, no. 12, pp. 2322–2333, 2013, doi: 10.1109/TMC.2012.190.

[14] J. Wilson and N. Patwari, "See-through walls: Motion tracking using variance-based radio tomography networks," *IEEE Trans. Mob. Comput.*, vol. 10, no. 5, pp. 612–621, 2011, doi: 10.1109/TMC.2010.175.

[15] Y. Zhao, N. Patwari, J. M. Phillips, and S. Venkatasubramanian, "Radio tomographic imaging and tracking of stationary and moving people via kernel distance," *IPSN 2013 - Proc. 12th Int. Conf. Inf. Process. Sens. Networks, Part CPSWeek 2013*, pp. 229–240, 2013, doi: 10.1145/2461381.2461410.

[16] Y. Zheng and A. Men, "Through-wall tracking with radio tomography networks using foreground detection," *IEEE Wirel. Commun. Netw. Conf. WCNC*, pp. 3278–3283, 2012, doi: 10.1109/WCNC.2012.6214374.

[17] N. Pirzada, M. Y. Nayan, F. S. M. F. Hassan, and M. A. Khan, "Device-free Localization Technique for Indoor Detection and Tracking of Human Body: A Survey," *Procedia - Soc. Behav. Sci.*, vol. 129, pp. 422–429, 2014, doi: 10.1016/j.sbspro.2014.03.696.

[18] F. Natterer and F. Wübbeling, "Mathematical methods in image reconstruction," *SIAM Monogr. Math. Model. Comput.*, vol. 107, no. 2002, pp. 1–207, 2001, doi: 10.1118/1.1455744.

[19] N. A. M. Ramli *et al.*, "A Design and Development of a Wireless Sensor Network for Potential Monitoring and Localization," *J. Electr. Eng. Technol.*, vol. 15, no. 6, pp. 2735–2743, 2020, doi: 10.1007/s42835-020-00515-5.

[20] C. Alippi, M. Bocca, G. Boracchi, N. Patwari, and M. Roveri, "RTI Goes Wild: Radio Tomographic Imaging for Outdoor People Detection and Localization," *IEEE Trans. Mob. Comput.*, vol. 15, no. 10, pp. 2585–2598, 2016, doi: 10.1109/TMC.2015.2504965.

[21] N. Kitbutrawat, H. Yamaguchi, and T. Higashino, "Easytrack: Zero-calibration smart-home tracking system," *J. Inf. Process.*, vol. 27, no. July, pp. 445–455, 2019, doi: 10.2197/ipsjjip.27.445.

[22] S. Koulouridis, "Device-Free Indoor Localization for AAL Applications," in *Lecture Notes of the Institute for Computer Sciences, Social-Informatics and Telecommunications Engineering*, 2012, vol. 83, no. November, pp. 399–402, doi: 10.1007/978-3-642-29734-2.

[23] J. F. Janek and J. J. Evans, "Predicting Ground Effects of Omnidirectional Antennas in Wireless Sensor Networks," *Wirel. Sens. Netw.*, vol. 02, no. 12, pp. 879–890, 2010, doi: 10.4236/wsn.2010.212106.

[24] I. Campbell Scientific, "Application Note: Line of Sight Obstruction," United Kingdom, 2016. [Online]. Available: https://s.campbellsci.com/documents/au/technical-papers/line-of-sight-obstruction.pdf.

[25] N. Mesto and C. R. Tel, "Ray Microwave link," Czech Republic, 2013. [Online]. Available: https://www.racom.eu/eng/products/m/ray/index.html.

[26] M. T. El Astal, "Fundamental Parameters of Antennas," 2011. doi: 10.1007/springerreference_22739.

[27] B. C. Capps and D. A. Systems, "Near field or Far field?" [Online]. Available: www.ednmag.com.

[28] V. Picchio, V. Cammisotto, F. Pagano, R. Carnevale, and I. Chimenti, "Atmospheric Attenuation due to Humidity," *Intechopen*, no. Cell Interaction-Regulation of Immune Responses, Disease Development and Management Strategies, pp. 1–15, 2020, [Online]. Available: https://www.intechopen.com/books/advanced-biometric-technologies/liveness-detection-in-biometrics.

[29] Honeywell, "Dielectric Constant Table," 2011. [Online]. Available: https://www.honeywellprocess.com/library/marketing/tech-specs/Dielectric Constant Table.pdf.

[30] M. Reuben and J. B. Frank, "The science and study of radio wave reflection, refraction, diffraction, absorption, polarization and scattering," in *WS&B*, 2011, pp. 1–75.